Journal of Combinatorial Mathematics
and Combinatorial Computing
www.combinatorialpress.com/jcmcc

Combinatorial Press

Computational methods for physiological signal data of heart failure patients and their predictive model design

Jinlong Zhuang[1], Taoming Qian[1], Li Liu[2,] ✉

[1] *Graduate School, Heilongjiang University of Traditional Chinese Medicine, Harbin, Heilongjiang, 150040, China*
[2] *The First Affiliated Hospital, Heilongjiang University of Traditional Chinese Medicine, Harbin, Heilongjiang, 150040, China*

ABSTRACT
ECG and PCG reflect the activity characteristics of the heart, and the combination of the two can record the electromechanical activity information of the heart more comprehensively. In this paper, we design a heart failure prediction model based on Transformer, and utilize Transformer Encoder to complete the feature fusion of ECG and PCG. Feature classification is performed using ResNet-18 to achieve the prediction of nine typical arrhythmias. Evaluate the classification results on the dataset to explore the performance level of the proposed model. Obtain ECG and PCG data in real situations, and select entropy analysis and heart rate variability metrics to quantify the physiological signal time series complexity. The model classification accuracy, specificity and sensitivity are compared to analyze the effect and superiority of the proposed model in practical applications. The results show that the average accuracy of the model on the four datasets reaches 92.28%, and the highest average F1 score is 0.930. In practical applications, the classification accuracy, specificity and sensitivity of the proposed model in this paper are 96.79%, 97.47% and 96.77%, respectively. Through the fusion analysis of ECG signal and heart sound signal characteristics, the model fully reflects the HRV change characteristics of heart failure patients and can effectively predict heart failure.

Keywords: heart failure, ECG, PCG, Transformer, feature fusion

1. Introduction

Heart failure is a group of syndromes in which various cardiac diseases develop to advanced stages, with a complex course, varying severity, and a high mortality rate in the context of quality of life, psychological status, nutritional indicators, and medical environment [1-4]. Heart failure can be caused by a variety of reasons, such as coronary heart disease, hypertension, myocarditis, and cardiomyopathy. Coronary heart disease causes myocardial ischemia, leading to impaired myocardial function [5]. Hypertension, on the other hand, increases the cardiac load, leading to cardiac

✉ Corresponding author.
E-mail address: valen333@126.com (L. Liu).
Received 01 March 2024; Revised 25 May 2024; Accepted 10 November 2024; Published Online 15 April 2025.
DOI: 10.61091/jcmcc127a-390

enlargement and hypertrophy, and ultimately causing heart failure [6]. And the physiologic manifestations of heart failure are not the same in different states. In terms of pathophysiology, heart failure is mainly characterized by decreased myocardial contractility and diminished diastolic function. Decreased myocardial contractility leads to a decrease in cardiac output and hypoxia of systemic organs, while diminished diastolic function leads to an increase in cardiac filling pressure, which further affects cardiac output [7-8]. In addition, heart failure is associated with complex pathophysiological changes such as myocardial remodeling and activation of the angiotensin-aldosterone-sympathetic nervous system [9-10].

In terms of clinical manifestations, heart failure often causes cardiac and pulmonary symptoms. Cardiac symptoms include shortness of breath, palpitations, fatigue, and intractable edema, while pulmonary symptoms are mainly characterized by dyspnea, cough, and sputum [11]. In addition, heart failure may also cause systemic manifestations such as liver function abnormalities and renal hypoplasia [12-13]. In terms of diagnosis, the diagnosis of heart failure mainly relies on clinical symptoms and signs, electrocardiogram, cardiac ultrasound and other auxiliary examinations, and clinically, heart failure is often categorized into acute and chronic heart failure according to the course of heart failure, and the clinical symptoms and treatments are also different [14]. Therefore, the physiologic signal data of heart failure patients are diverse and complex. With the development of technology, doctors issuing treatment plans and diagnosis no longer rely only on doctors' personal experience, but with the help of intelligent technology, the patient's physical data are analyzed to assist doctors and caregivers in diagnosis, treatment and rehabilitation care [15-17]. In order for doctors to better understand the physiological status of heart failure patients and subsequent diagnostic and therapeutic judgment, it is necessary to develop a calculation method and prediction model suitable for the physiological signal data of heart failure patients.

In this paper, we first introduce the data sources of the study and propose the pre-processing method of ECG signal data. A heart failure prediction model based on Transformer was designed to transform PCG signals using MFCC and feature extraction using Transformer Encoder. Higher order ECG and PCG features are fused and classification of hybrid features is achieved with the help of ResNet-18. Classification prediction is performed on the divided dataset using the proposed model, and the performance level is visualized relying on the confusion matrix. The actual ECG and PCG data are collected, and the entropy-based physiological signal feature quantization method is proposed. The proposed model is compared with existing automatic prediction models for heart failure to verify its effectiveness in practical applications.

2. Transformer-based heart failure prediction algorithm

2.1. Data composition and processing

ECG, as the most commonly used auxiliary diagnostic method for cardiac diseases, contains rich information about heart beats and clinical features. Classification of arrhythmias based on ECG signals is an important analysis method for accurate detection, effective treatment and timely warning of various heart failure diseases. This section describes the preprocessing methods of ECG signal data to prepare the preliminary data for the establishment of heart failure prediction models.

2.1.1. Data sources and groupings. A total of 16,000 12-lead ECG recordings in mat format were used in this study, which varied in noise level, sequence length and amplitude range. Before designing the structure of the neural network, it is necessary to process the data briefly using some mathematical methods. In this work, the ECG co-labeled by several cardiologists consists of 8000 12-lead ECG records with a sampling rate of 500 Hz. is divided into three parts, 6250 records as a training set, 950 records as a validation set, and 800 records as a test set #1. Each record may have multiple different arrhythmia labels, so one record can be counted repeatedly in the respective statistics of different

labels. To make the results more convincing, 7200 ECG records collected from multiple sources were used as test set No. 2, which has the same amount of data as the training and validation sets combined, and 800 ECG records collected from the PhysioNet public database were used as test set No. 3. Test set No. 2 can effectively illustrate the generalization of the model obtained from the training due to the mixing and wide range of data sources; Test set #3 facilitates controlled experiments due to the public nature of the data. The number of ECG records corresponding to each of the nine types of arrhythmias is shown in Table 1.

Table 1. Data set partitioning details

Type	Trainset	Valset	Test set1	Test set2	Test set3
Normal	1848	274	183	2018	285
AF	504	69	59	649	58
FDAVB	523	76	63	562	52
CRBBB	805	98	84	863	61
LAFB	166	39	45	219	39
PVC	617	84	79	705	68
PAC	628	80	61	692	75
ER	205	22	18	325	17
TWC	2088	195	184	2359	173
Total	6250	950	800	7200	800

2.1.2. ECG signal denoising. ECG signal has the characteristics of low frequency, instability and strong ability to accept interference, which leads to the collection process of ECG signal will inevitably be affected by a variety of interfering information, and these interfering information, if more, will even cover up some useful information in the original ECG signal. In order to better utilize the effective information of ECG signals, denoising of ECG signals is required.

Wavelet transform can analyze the signal in the time domain frequency domain at the same time, especially in one-dimensional signal processing noise, detection of feature points has good ability, it has become a commonly used method to remove noise in recent years, the ECG signal containing noise can be expressed by formula (1):

$$s(t) = f(t) + \sigma \cdot e(t) t = 0,1,\cdots,n-1 \tag{1}$$

where $f(t)$ is the real ECG signal, $e(t)$ denotes the noise, $s(t)$ denotes the ECG signal mixed with noise and σ denotes the standard deviation of the noise. The denoising process of wavelet transform is;

1) First process the ECG signal containing noise by wavelet decomposition: choose a wavelet basis function, specify the number of decomposition layers as N, and then perform N-layer decomposition of the signal; according to the characteristics of the ECG signal, the commonly used wavelet basis functions to process the ECG signal are the four kinds of Hear, Daubechies6, Symmlet8, and Coiflets5;

2) Quantizing the decomposed high-frequency coefficients: that is, determining a suitable threshold for the high-frequency coefficients from the first to the last layer, and then quantizing them;

3) Reconstructing the signal: based on the wavelet decomposition of the high frequency coefficients of each layer from the front to the back and the low frequency coefficients of the last layer to reconstruct the process.

The most critical step in denoising by wavelet transform is the selection of threshold, which, to a certain extent, can reflect the effect of noise removal. After applying a small threshold, the wavelet coefficients will contain too many noise components, which may not achieve the effect of filtering; a large threshold may lose the effective components of the ECG signal, resulting in the loss of the original

characteristics of the signal. In this section, the very large and very small threshold method is used to determine the size of the threshold. The method is to minimize the great variance obtained by selecting the threshold value, and is able to find the threshold value by calculating the minimum value of the variance of the signal after filtering and the original signal in the worst case.

2.2. Modeling

2.2.1. Transformer Encoder. Transformer is a popular neural network architecture for processing sequential data, especially performing well in natural language processing tasks.The Transformer architecture consists of two parts, Encoder and Decoder, where Encoder mainly uses multi-head self-attention to extract and uplift the overall features from the context of the input data sequence to transform the The input sequence is encoded into a fixed-length high-dimensional feature vector representation, while the Decoder is used to generate the target sequence. The structure of a single Transfomer Encoder is shown in Figure 1.

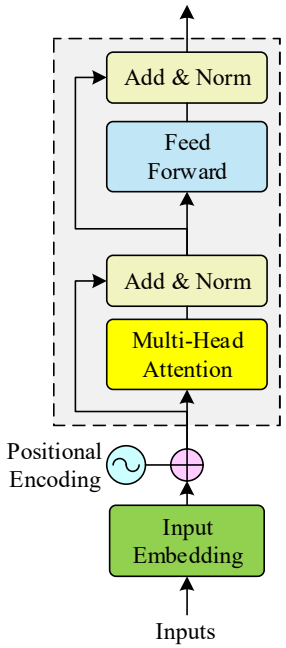

Fig. 1. Structure of a single Transformer Encoder

2.2.2. Algorithmic Model. For preprocessing, the model transforms the PCG signal using the Mel Falling Spectral Coefficient (MFCC), which is more in line with the auditory properties of the human ear and still has good recognition performance when the signal-to-noise ratio is reduced. Then, a one-dimensional convolutional neural network is used for feature pre-extraction, and then its initial-order features are deeply extracted using Transformer Encoder to obtain the higher-order features after Encoder. Finally, the higher-order ECG and PCG features are fused and mixed with Gaussian noise in the third dimension and classified using ResNet-18.

The model performs initial feature extraction on the preprocessed ECG and PCG spectral sequences using a one-dimensional convolutional neural network with two-dimensional convolutional kernel (ID-CNN), which effectively matches the input data and performs appropriate data compression. 1D-CNN is mainly used in the field of processing time series data, signals, etc. Compared with the traditional signal processing methods, it can automatically learn the features in the data, avoiding the tedious process of manually extracting features. The main roles of the 1D-CNN layer in the model are feature pre-extraction, data compression and dimension matching.

The 1D-CNN neural network layer performs convolutional operations in a single dimension, and its convolutional computation is shown in Fig. 2.The modeled ID-CNN uses a two-dimensional convolutional kernel that performs convolutional operations along the time dimension. It has a set of self-learning convolution kernels that are commonly used for feature compression and high-dimensional mapping with the following formula:

$$O = \frac{Input - K}{S} + 1 \tag{2}$$

$$O(t) = \sum_{a=-\infty}^{\infty} x(a)\omega(t-a) \tag{3}$$

where $O(t)$ is the compressed data, $x(a)$ is the data from the input port, and $\omega(t-a)$ is the convolutional kernel function.The ID-CNN is compressed in the temporal dimension of the PCG, mapped to match the ECG, and appropriately enhances the temporal length of the ECG. Then, each channel PCG and ECG are deep mined and encoded independently for each modal feature using Transformer Encoder based on multi-head self-attention and residual connection, with the feature vector length of 204, the number of feed-forward network weights in the Encoder layer of 2048, and the number of Encoder layers is 3.

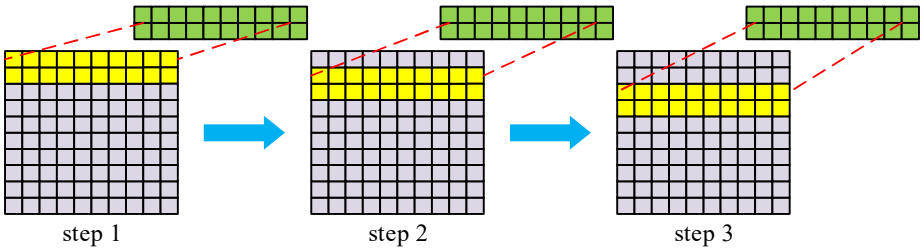

Fig. 2. Calculation of 1D-CNN

The output of the Encoder layer is two deeply encoded feature matrices, where we blend them with Gaussian noise in the third channel to form a $3\times204\times length$ fusion matrix. Gaussian noise is a class of noise whose probability density function obeys a Gaussian distribution, and blending them into features improves the generalization ability of the neural network. In the final stage of the model, the blended features are classified using ResNet-18 and the values of the neurons are output through a linear layer of 512×1 and a Sigmoid activation function.

2.3. Performance evaluation

According to the experimental procedure, the model is constructed, the parameters are trained, and the results are evaluated on the dataset that has been divided, and then try to solve the prediction problem of heart failure and health with the model proposed in this paper.

The confusion matrix plotted based on the best classification results from the validation set (set1) is shown in Figure 3. The samples on the main diagonal line account for the majority of the errors, and the few errors occur mainly in the surrounding regions. There is a strong correlation between interclass morphological similarity and interclass confusion, and most of the abnormally distributed samples are explainable. For example, the reason for the large number of false-positive samples of the normal type is that all null predictions below a defined threshold are deliberately categorized as Normal. the model achieves an accuracy of 94.35%, incorrectly predicts 13 normal samples as TWC, and TWC is also confounded with the other seven types to varying degrees, partly because the convolution and pooling operations have caused the important minor fluctuation information to be eliminated. It can also be seen that the negative effects of false-positive and false-negative samples are

amplified on the ER, partly due to the extreme imbalance of the ECG record of the ER, and partly due to the inability of the model to efficiently learn the degree of J-point elevation.

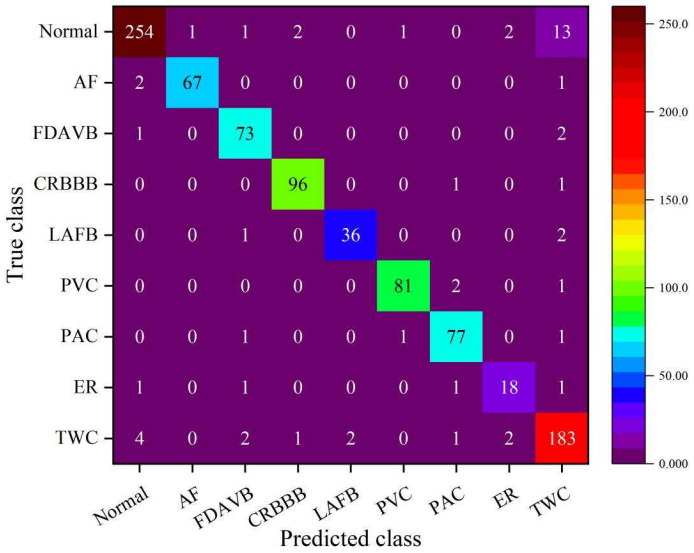

Fig. 3. Confusion matrix on the validation set

The confusion matrix for the test set is shown in Fig. 4, where the model incorrectly predicted 16 other samples as TWC in test set #2, 560 TWC samples as other samples in test set #3, and 37 samples were generated by the confusion of TWC with other types in test set #4, but overall the model accuracy reached 94.33%, 87.47%, and 92.95%, respectively, which proves that the resulting model generalization performance is good.

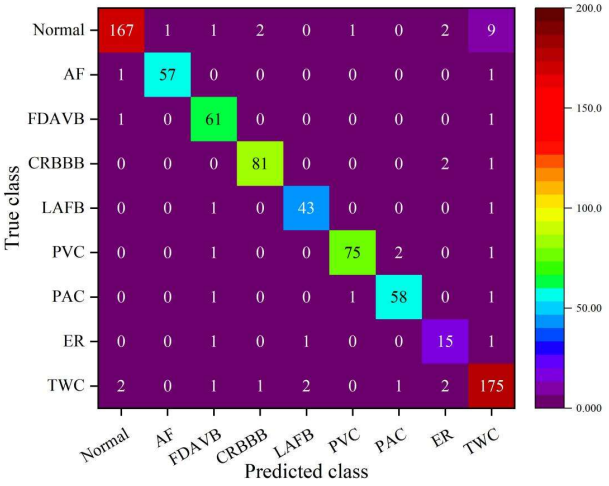

(a)Test set 2

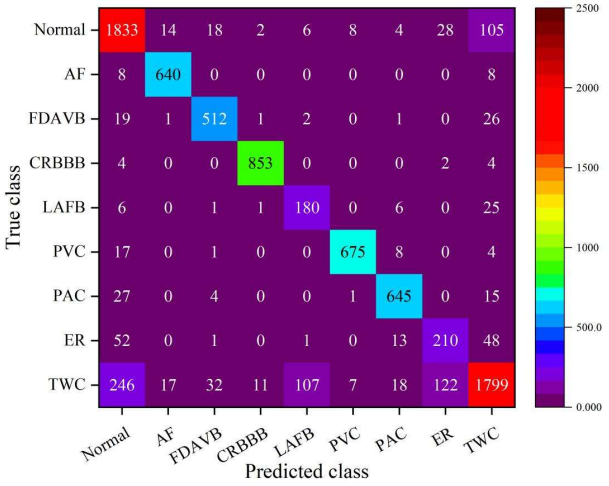

(b)Test set 3

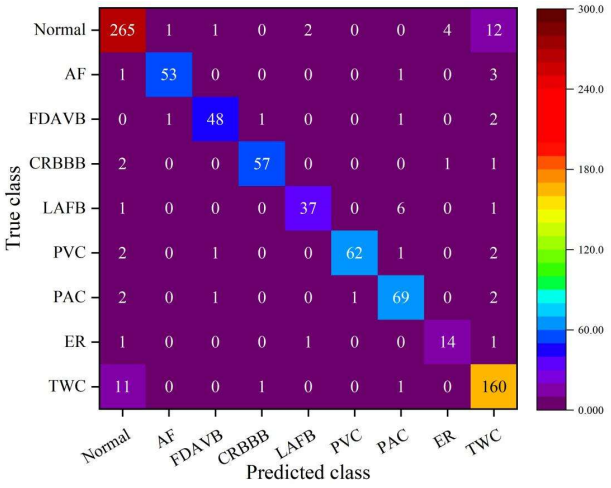

(c)Test set 4

Fig. 4. Confusion matrix on the testing set

The learning effect of the model is outstanding from the point of view of the confusion matrix. In order to have an objective and comprehensive understanding of the model, this paper calculates the checking accuracy, checking completeness, specificity and F1 scores of nine categories on the validation set (set1) and three test sets (set2, set3, set4), and the results of the tests are shown in Table 2.The average F1 score is the highest at 0.930, and the lowest at 0.906.It can be clearly seen that AF, FDAVB, CRBBB, PVC, and PAC have stable scores in the four datasets and have strong generalization ability. When the number of test samples increases to 7200 (set3), the confusion between Normal and TWC classes increases. The extremely limited number of LAFBs and ERs in the training set posed an overfitting risk to the model, and the F1 scores of the two classes achieved with a more diverse test set decreased significantly.

Table 2. The composite performance of the model over different data sets

		Normal	AF	FDAVB	CRBBB	LAFB	PVC	PAC	ER	TWC	Average
Precision (PPV)	Set1	0.903	0.976	0.936	0.972	0.903	0.966	0.921	0.774	0.935	0.921
	Set2	0.929	0.968	0.934	1.000	0.924	0.953	0.923	0.732	0.911	0.919
	Set3	0.894	0.970	0.941	0.983	0.919	0.963	0.908	0.684	0.875	0.904
	Set4	0.883	0.983	0.929	0.974	0.921	0.973	0.912	0.698	0.891	0.907
Recall	Set1	0.963	0.981	0.898	0.992	0.906	0.963	0.874	0.793	0.863	0.915
	Set2	0.958	0.974	0.875	1.000	0.902	0.960	0.883	0.758	0.893	0.911
	Set3	0.961	0.983	0.894	0.994	0.893	0.983	0.847	0.694	0.849	0.900
	Set4	0.946	0.979	0.886	0.987	0.891	0.971	0.865	0.784	0.864	0.908
Specificity	Set1	0.961	0.997	0.997	0.996	0.993	0.995	0.996	0.995	0.948	0.986
	Set2	0.963	0.998	0.998	1.000	0.989	0.976	0.994	0.993	0.979	0.988
	Set3	0.959	0.996	0.998	0.997	0.995	0.974	0.961	0.974	0.992	0.983
	Set4	0.958	0.997	0.996	0.998	0.996	0.983	0.992	0.989	0.958	0.985
F1 score	Set1	0.943	0.984	0.925	0.984	0.903	0.969	0.901	0.793	0.904	0.923
	Set2	0.938	0.978	0.918	1.000	0.982	0.967	0.898	0.768	0.918	0.930
	Set3	0.874	0.983	0.914	0.981	0.989	0.961	0.903	0.694	0.858	0.906
	Set4	0.893	0.982	0.911	0.979	0.981	0.970	0.905	0.728	0.874	0.914

3. Example analysis of heart failure disease prediction based on fusion of ECG and PCG features

3.1. Actual signal acquisition and processing

In order to obtain multi-physiological signal data in real situations, this study performed signal acquisition on the subjects, which can get the corresponding ECG and heart sound data and save them. The subjects were kept in a sedentary and stable state during the measurement process to minimize the effects of small movements. The subjects in this study were divided into healthy and abnormal groups, ten in each group.

The received ECG signals are shown in Figure 5.

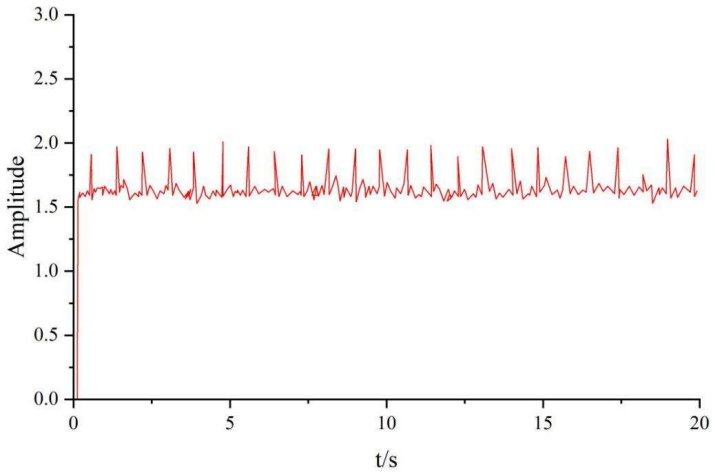

Fig. 5. ECG signal

The heart sound signal obtained from sampling is shown in Figure 6.

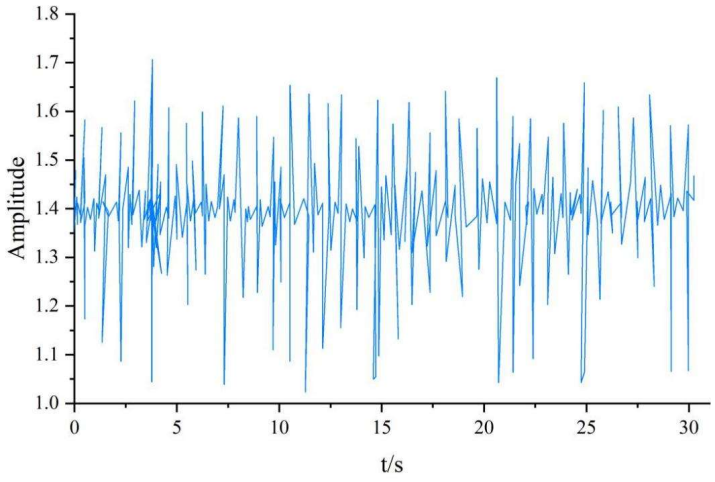

Fig. 6. PCG signal

3.2. Quantification of physiological signal data

Entropy analysis is very effective in quantifying the complexity of the ECG signal time series; in general, the lower the entropy value of the heart rate variability (HRV) signal, the lower the complexity of the time series, i.e., the lower the cardiac function. Sample entropy is a statistical calculation used to estimate the complexity of biological time series signals. Alignment entropy is a measure of system

complexity derived from dynamical systems theory. In this paper, sample entropy and alignment entropy are used to extract the characteristics of complexity of HRV signals, respectively.

The sample entropy is calculated as follows: a segment of the HRV signal time series is selected as $y=\{y_1,y_2,y_3,...,y_{N-1},y_N\}$, and it is constituted as a m-dimensional vector, i.e:

$$Y_t^m=\{y_t,y_{t+1},...,y_{t+m-2},y_{t+m-1}\} \tag{4}$$

Eq. $t=1,2,...N-(m+1)$.

Define the distance between Y_{t1}^m and Y_{t2}^m as $d\left[Y_{t1}^m,Y_{t2}^m\right]$ (t_1 is not equal to t_2), as the one with the largest difference between the two corresponding elements i.e:

$$d\left[Y_{t1}^m,Y_{t2}^m\right]=\max_{k\in(0,m-1)}\left|Y_{t1+k}^m-Y_{t2+k}^m\right| \tag{5}$$

Given a threshold value of $r(r>0)$, count the number of $d\left[Y_{t1}^m,Y_{t2}^m\right]<r$ and ratio them to the total number of vectors, ie:

$$B_t^m(r)=\frac{1}{N-m}num\left\{d\left[Y_{t1}^m,Y_{t2}^m\right]<r\right\} \tag{6}$$

For averaging all the results obtained from Eq. (4), i.e:

$$B^m(r)=\frac{1}{N-m+1}\sum_{t=1}^{N-m+1}B_t^m(r) \tag{7}$$

Then the sample entropy of this sequence is:

$$SampEn(y,m,r)=-\ln\left[\frac{B^{m+1}(r)}{B^m(r)}\right] \tag{8}$$

Its arrangement entropy is calculated as follows:

A time series X of length N is selected for phase space reconstruction to obtain a matrix Y as:

$$Y=\begin{bmatrix} x(1) & x(1+t) & \cdots & x(1+(m-1)t) \\ \vdots & \vdots & & \vdots \\ x(j) & x(j+t) & \cdots & x(j+(m-1)t) \\ \vdots & \vdots & & \vdots \\ x(K) & x(K+t) & \cdots & x(K+(m-1)t) \end{bmatrix} \tag{9}$$

where m is the embedding dimension, t is the delay time, and $K=N-(m-1)t$. Each reconstructed component is rearranged in ascending order to obtain a set of symbolic sequences formed by the column indices of the positions of the elements in the vector.

$$S(l)=\{j_1,j_2,...,j_m\} \tag{10}$$

where $l=1,2,...,k$ and $k\le m!$.

There are a total of $m!$ different symbol sequences for the m-dimensional phase space mapping. Calculate the number of occurrences of each symbol sequence divided by the total number of occurrences of the $m!$ different symbol sequences as the probability of occurrence of that symbol sequence. That is $\{P_1,P_2,...,P_k\}$.

The entropy of the permutation of time series X is calculated as:

$$H_p(m)=-\sum_{j=1}^{k}P_j\ln P_j \tag{11}$$

Sample entropy and alignment entropy are measures of the complexity of the time series and the size of the probability of the sequence generating a new pattern when the dimensionality changes; the greater the probability of generating a new pattern, i.e., the greater the complexity of the time series, the greater the value, and conversely, the smaller the value, which indicates that the time series is simpler and more regular. The mean values of both sample entropy and alignment entropy of normal people are larger than those of patients with heart failure diseases, which is in line with the theory that the time series of ECG signals of normal people are more complex and random.

Comparison of the distribution of sample entropy and alignment entropy values between normal people and patients with heart failure diseases is shown in Figure 7. As can be seen from Fig. 7, the mean value of the sample entropy of normal people and patients with heart failure is more different, and the distribution of the arrangement has less overlapping parts.

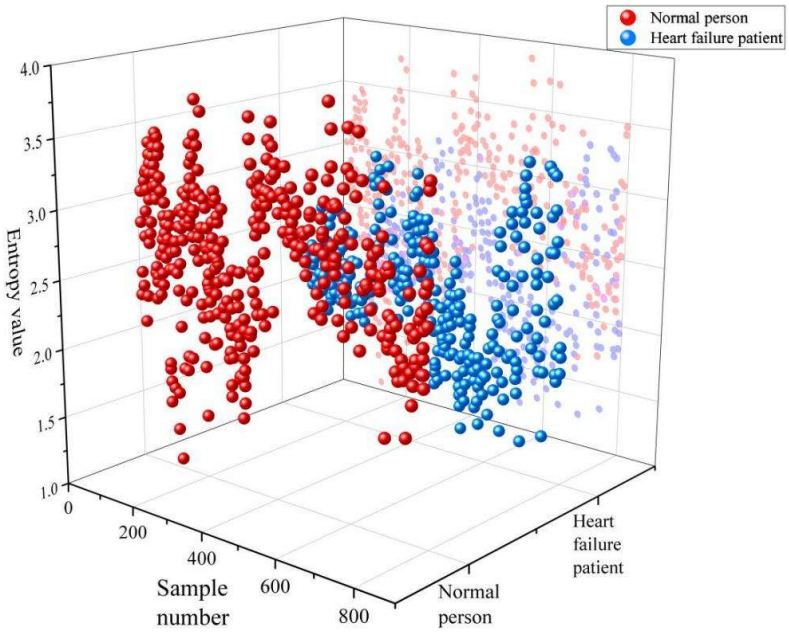

(a)Sample entropy

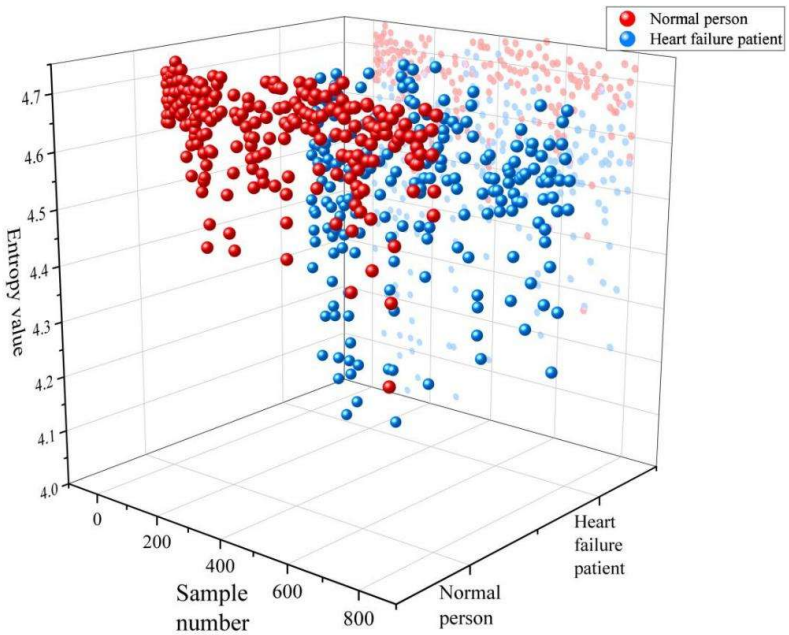

(b)Permutation entropy

Fig. 7. Distribution of entropy values in normal subjects and patients with HF

Based on the different properties of the two features, the two entropy features are fused. The distribution after the fusion of the two is shown in Fig. 8, which shows that the fusion of the two features can better distinguish between normal people and patients with heart failure diseases.

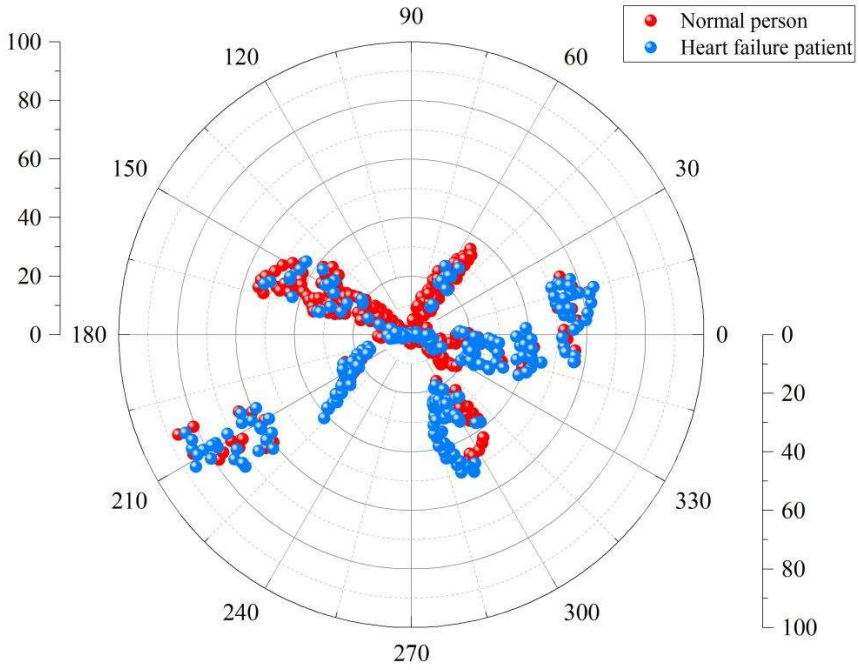

Fig. 8. Feature fusion distribution of sample entropy and permutation entropy

3.3. Comparative analysis of forecast results

In order to verify the effectiveness of the Transformer-based prediction method for heart failure patients proposed in this paper for practical applications, it was compared with existing automatic prediction models for heart failure.

The six control models are numbered as A~F, and the specific testing methods are described below.

Model A: The method of combining CNN and DDM for entropy calculation, using the entropy method to generate the DDM, and then using the CNN model to learn the data distribution pattern hidden in the DDM.

Model B: Extracting time-frequency domain and wavelet entropy features, using KNN classifier, and evaluating feature performance.

Model C: Extract time domain and wavelet transform based frequency domain features and use backward elimination for feature selection and finally classify using SVM classifier.

Model D: Extraction of time-domain, frequency-domain and wavelet entropy features and feature selection using genetic algorithm and finally evaluation using KNN classifier.

Model E: Extract two time domain and Renyi entropy, put the features into classifiers such as Park Bayes, KNN and Decision Tree for classification.

Model F: Three time domain features, three frequency domain features and three nonlinear features are extracted and classified using SVM classifier.

The comparison results are shown in Table 3. The specificity of model D reaches 99.54%, but the sensitivity is only 80.32%. The classification accuracy, specificity and sensitivity of the model proposed in this paper are 96.79%, 97.47% and 96.77%, respectively. Compared with other algorithms, the model proposed in this paper, which analyzes the multi-scale features of the time series, achieves an advantage in terms of accuracy and sensitivity, and by fusing and analyzing the features of ECG signals

and cardiac sound signals, it adequately reflects the characteristics of the HRV changes in the heart failure patients.

Table 3. Comparison of prediction models for heart failure

Model	Accuracy rate	Specificity	Sensitivity
A	80.53%	87.35%	69.11%
B	87.35%	93.24%	77.43%
C	89.14%	95.08%	80.65%
D	92.19%	99.54%	80.32%
E	85.98%	79.43%	92.30%
F	90.11%	89.01%	90.18%
The proposed	96.79%	97.47%	96.77%

4. Conclusion

In this paper, we propose a Transformer-based heart failure prediction model to investigate its performance level and practical application.

In the validation set, the model incorrectly predicts 13 normal samples as TWC, and TWC is also confounded with the other seven types to varying degrees.The accuracy of the model on test set 1, test set 2, and test set 3 reaches 94.33%, 87.47%, and 92.95%, respectively, which proves that the resulting model has good generalization performance. On the four datasets, the highest average F1 score is 0.930, and the scores of AF, FDAVB, CRBBB, PVC, and PAC are stable, and when the number of test samples is increased to 7,200 (set3), the confusions between the Normal and TWC classes increase.

In practical application, the specificity of Model D among the six models reaches 99.54%, but the sensitivity is only 80.32%. The classification accuracy, specificity and sensitivity of the model proposed in this paper are 96.79%, 97.47% and 96.77%, respectively. Compared with other algorithms, the model of this paper achieves an advantage in accuracy and sensitivity, and the difference of the three indexes is small. The model in this paper fully reflects the characteristics of HRV changes in heart failure patients through the fusion analysis of ECG signal and heart sound signal characteristics.

Funding

This work was supported by Science and Technology Innovation team of Heilongjiang University of Traditional Chinese medicine (2019TD01).

References

[1] Johansson, I., Joseph, P., Balasubramanian, K., McMurray, J. J., Lund, L. H., Ezekowitz, J. A., ... & G-CHF Investigators. (2021). Health-related quality of life and mortality in heart failure: the global congestive heart failure study of 23 000 patients from 40 countries. Circulation, 143(22), 2129-2142.

[2] Shen, B. J., Xu, Y., & Eisenberg, S. (2017). Psychosocial and physiological predictors of mortality in patients of heart failure: Independent effects of marital status and C-reactive protein. International journal of behavioral medicine, 24, 83-91.

[3] Yoshihisa, A., Kanno, Y., Watanabe, S., Yokokawa, T., Abe, S., Miyata, M., ... & Takeishi, Y. (2018). Impact of nutritional indices on mortality in patients with heart failure. Open heart, 5(1), e000730.

[4] Ajayi, A. A., Sofowora, G. G., & Ladipo, G. O. (2020). Explaining heart failure hyper-mortality in sub saharan Africa: global genomic and environmental contribution review. Journal of the National Medical Association, 112(2), 141-157.

[5] Bansal, N., Katz, R., Robinson-Cohen, C., Odden, M. C., Dalrymple, L., Shlipak, M. G., ... & de Boer, I. H. (2017). Absolute rates of heart failure, coronary heart disease, and stroke in chronic kidney disease: an analysis of 3 community-based cohort studies. JAMA cardiology, 2(3), 314-318.

[6] Slivnick, J., & Lampert, B. C. (2019). Hypertension and heart failure. Heart failure clinics, 15(4), 531-541.

[7] Tschöpe, C., Kherad, B., Klein, O., Lipp, A., Blaschke, F., Gutterman, D., ... & Van Linthout, S. (2019). Cardiac contractility modulation: mechanisms of action in heart failure with reduced ejection fraction and beyond. European journal of heart failure, 21(1), 14-22.

[8] Obokata, M., Reddy, Y. N., & Borlaug, B. A. (2020). Diastolic dysfunction and heart failure with preserved ejection fraction: understanding mechanisms by using noninvasive methods. JACC: Cardiovascular Imaging, 13(1 Part 2), 245-257.

[9] Aimo, A., Gaggin, H. K., Barison, A., Emdin, M., & Januzzi, J. L. (2019). Imaging, biomarker, and clinical predictors of cardiac remodeling in heart failure with reduced ejection fraction. JACC: Heart Failure, 7(9), 782-794.

[10] Varghese, T. P., & Tazneem, B. (2024). Unraveling the complex pathophysiology of heart failure: insights into the role of renin-angiotensin-aldosterone system (RAAS) and sympathetic nervous system (SNS). Current Problems in Cardiology, 49(4), 102411.

[11] Akanda, M. A. K. (2025). Pattern And Clinical Manifestation Of Heart Failure A Case Distribution Analysis Of 872 Cases From A Heart Failure Clinic In Bangladesh. Journal of Cardiac Failure, 31(1), 239.

[12] Drăghici, T., Negreanu, L., Bratu, O. G., Tincu, R., Socea, B., Iancu, M. A., ... & Diaconu, C. (2018). Liver abnormalities in patients with heart failure. Archives of the Balkan Medical Union, 53(1), 76-81.

[13] Clark, A. L., Kalra, P. R., Petrie, M. C., Mark, P. B., Tomlinson, L. A., & Tomson, C. R. (2019). Change in renal function associated with drug treatment in heart failure: national guidance. Heart, 105(12), 904-910.

[14] Authors/Task Force Members:, McDonagh, T. A., Metra, M., Adamo, M., Gardner, R. S., Baumbach, A., ... & Waltenberger, J. (2022). 2021 ESC Guidelines for the diagnosis and treatment of acute and chronic heart failure: Developed by the Task Force for the diagnosis and treatment of acute and chronic heart failure of the European Society of Cardiology (ESC). With the special contribution of the Heart Failure Association (HFA) of the ESC. European journal of heart failure, 24(1), 4-131.

[15] Chui, K. T., Alhalabi, W., Pang, S. S. H., Pablos, P. O. D., Liu, R. W., & Zhao, M. (2017). Disease diagnosis in smart healthcare: Innovation, technologies and applications. Sustainability, 9(12), 2309.

[16] Moses, J. C., Adibi, S., Angelova, M., & Islam, S. M. S. (2022). Smart home technology solutions for cardiovascular diseases: a systematic review. Applied System Innovation, 5(3), 51.

[17] Bergier, H., Duron, L., Sordet, C., Kawka, L., Schlencker, A., Chasset, F., & Arnaud, L. (2021). Digital health, big data and smart technologies for the care of patients with systemic autoimmune diseases: where do we stand?. Autoimmunity reviews, 20(8), 102864.